# Noise Analysis of Analog Correlator *

Tu Chunjiang, Liu Bo'an, and Chen Hongyi

(*Institute of Microelectronics, Tsinghua University, Beijing* 100084, *China*)

**Abstract:** A noise model for the analog correlator used in the ultra wideband receivers is proposed due to lack of simulation capability on noise performance of the correlator in current EDA tools. The analog correlator circuit is divided into several parts to calculate the equivalent noise sources respectively. The ideal impulse generators, instead of the noise sources, are then applied to obtain the time varying transfer functions. Fourier transforms are carried out to explore the relationship between the noise input and output in frequency domain for each part. Then the symmetrical noise sources are grouped together and the periodicity of the circuit is utilized to further simplify the model. This model can be used to evaluate noise performance of the correlator.

**Key words:** noise; correlator; analog
**EEACC:** 1205; 1150
**CLC number:** TN431.1 **Document code:** A **Article ID:** 0253-4177(2005)03-0480-07

## 1 Introduction

Ultra wideband (UWB) communication systems which use modulated short impulses in their physical layer have been drawing increasing attention in recent years. They transmit information through short pulses in contrast with traditional wireless communication systems using sinusoidal carriers. Fewer components and hence less power consumption are required for the front-end[1], where a correlator is an indispensable component for signal detection in the receiver[2]. A new 3～10 GHz analog correlator, consisting of a standard Gilbert cell and a load capacitor, was described in Ref. [3]. In order to estimate the noise figure of the circuit, a new noise model has been developed because currently there is no EDA tool which can simulate the noise performance of analog correlator. The noise model is based on the theory of the linear time-varying (LTV) systems. The symmetrical and differential structure of the circuit is explored in the model. The quasi-periodicity of the circuit in one symbol is also utilized to further simplify the model.

## 2 Correlator

Correlation is an effective technique to detect the presence of signals with known waveforms in noisy background, especially in pulse-communication systems[2]. The design of the correlator carrying out this task has been given in Ref. [3]. The cross correlation function can be described as $f$ =

* Project supported by National High Technology Research and Development Program of China (No. 2003AA123210)

Tu Chunjiang male, was born in 1977, PhD candidate. His main research interests are circuits and system design of wireless communications.

Liu Bo'an male, was born in 1961, associate professor. His current research interests are VLSI implementation of wireless communication system and neural networks application.

Chen Hongyi male, was born in 1942, professor. His research interests are semiconductor device structures and integrated circuit design, ASIC and SOC (system on a chip) design methodology, algorithm mapping to hardware architecture and realization, VLSI DSP and applications in multimedia signal processing and information security field.

Received 3 August 2004, revised manuscript received 12 October 2004

$\int_{t_0}^{t_0+T} \mathrm{RF}(t)\mathrm{LO}(t)\,\mathrm{d}t$, where LO ($t$) is the local template signal, RF($t$) is the input radio frequency signal of the correlator, and $T$ is the integration period. The schematic of the correlator is shown in Fig. 1, including a pre-distortion (PD) circuit, a Gilbert cell (GC), and a common mode feedback (CMFB). The PD and GC multiply RF and LO and then integrate the result via a capacitor. The circuit is designed based on IBM 0.24μm SiGe BiCMOS technology, which has 47 GHz of highest transient frequency $f_T$ for npn HBT transistors.

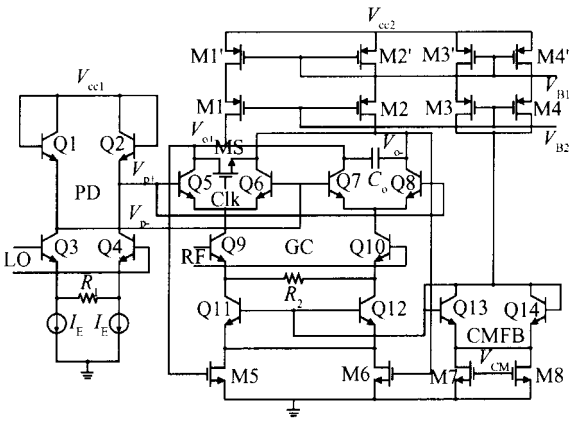


Fig. 1　Schematic of correlator

## 3　Noise model

### 3.1　Theory

As the LO signal changes with time, the correlator can be treated as a LTV system. The relation between the input and output of a LTV system is[4] $y(t) = \int_{-\infty}^{\infty} h(t,\tau)\,x(\tau)\,\mathrm{d}\tau$, where $h(t,\tau)$ is the response excited by an impulse launched at time $\tau$, $x(t)$ and $y(t)$ represent the input and output, respectively. In the frequency domain, the relation can be described by[5]

$$Y(\omega) = \int_{-\infty}^{\infty} H(\omega,\omega_t)\,X(\omega_t)\,\mathrm{d}\omega_t \qquad (1)$$

where $H(\omega,\omega_t) = \frac{1}{2\pi}\int_{-\infty}^{\infty}\int_{-\infty}^{\infty} h(t,\tau)\,\mathrm{e}^{\mathrm{j}\omega_t\tau}\mathrm{e}^{-\mathrm{j}\omega t}\,\mathrm{d}\tau\mathrm{d}t$, $X(\omega_t)$ and $Y(\omega)$ are the Fourier transforms of $x(t)$ and $y(t)$, respectively.

#### 3.1.1　Single input port

If a stationary stochastic process is applied at the input of a periodical LTV system, the output is cyclostationary. Thereby the randomly shifted process of the output is a stationary process, whose power spectrum density (PSD) can be used to describe the spectrum property of the output process. Although the LO signal is not periodical in terms of pulse, it is periodical in terms of symbol. Therefore the theory of a periodical LTV system can still be applied for the correlator. By Eq. (1), the noise PSD of the output can be derived as[5]

$$S_o(\omega) = \sum_{n=-\infty}^{\infty} |\,H_n(\omega)\,|^2 S(\omega + n\omega_s) \qquad (2)$$

where $S(\omega)$ stands for the PSD of the input source, $H_n(\omega)$ is the two-dimensional Fourier transform of the impulse response $h(t,\tau)$ and is given by

$$H_n(\omega) = \int_{-\infty}^{\infty}\left[\frac{1}{T_s}\int_0^{T_s} g(t,\tau)\,\mathrm{e}^{-\mathrm{j}n\omega_s\tau}\,\mathrm{d}\tau\right]\mathrm{e}^{-\mathrm{j}\omega t}\,\mathrm{d}t,\quad 0 < \tau \le T_s \qquad (3)$$

$g(t,\tau) \equiv h(t+\tau,\tau)$, $T_s$ denotes symbol period ($\omega_s = 2\pi/T_s$). The physical representation of $g(t,\tau)$ is the impulse response observed at a relative time after the launch of the impulse at time $\tau$.

An example of the waveform of the LO signal is illustrated in Fig. 2, where it is composed of several positive and negative pulses (chips), and $T_s$ and $T_c$ denote the symbol and chip period, respectively. The value of the chips (1: positive pulse, 0: negative pulse) in one symbol is determined by the predefined spreading codes. Let $t_1$ and $t_2$ denote any two time points when the pulses of the LO signal have the same polarity. If $|t_1 - t_2|$ is integral times of $T_c$, as shown in Fig. 2, the coefficient matrices of the state variable equation (SVE) have the same value at $t_1$ and $t_2$, which has been proved in the Appendix. Based on the above conclusions, the impulse response $g(t,\tau)$ can be divided into several independent impulse responses along $\tau$ axis, corresponding to every pulse (chip) of the LO signal in one symbol. Therefore $g(t,\tau)$ can be expressed as

$$g(t,\tau) = \sum_{k\in A} g_+(t,\tau - kT_c) + \sum_{k\in A} g_-(t,\tau - kT_c),$$

where both $\mathbf{A}$ and $\overline{\mathbf{A}}$ are integer sets which stand for the indices for positive pulses and negative pulses in one symbol, respectively. Let $N$ denote the spreading factor in direct-sequence UWB system, i. e. $N = T_s/T_c$, then $\mathbf{A} \cap \overline{\mathbf{A}} = \{0, 1, \cdots, N-1\}$ and $k \in \{0, 1, \cdots, N-1\}$. If the stimulation impulse is launched when the chip value of the LO signal is 1 or 0, the impulse response of the correlator is denoted by $g_+(t, \tau')$ or $g_-(t, \tau')$, respectively, as shown in Fig. 2. $\tau'$ is the impulse launch time and $g_\pm(t, \tau') = 0$ when $\tau' < 0$ or $\tau' \geq T_c$.

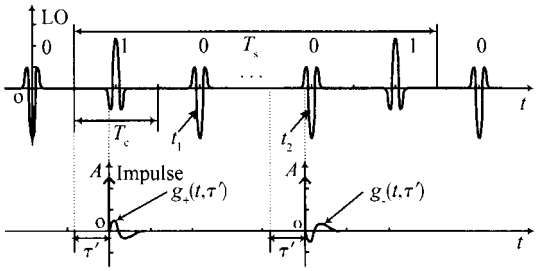


Fig. 2 Waveform of LO signal

Therefore the Fourier transform of $g(t, \tau)$ in terms of time $t$ can also be derived according to the different value of $\tau$, shown by the following equation $G(\omega, \tau) = \sum_{k \in \mathbf{A}} G_+(\omega, \tau - kT_c) + \sum_{k \in \overline{\mathbf{A}}} G_-(\omega, \tau - kT_c)$, where $G_+(\omega, \tau')$ and $G_-(\omega, \tau')$ are the Fourier transforms of $g_+(t, \tau')$ and $g_-(t, \tau')$ respectively. If we change the integral order of $t$ and $\tau$ in Eq. (3) and use the above equation, we obtain

$$H_n(\omega) = \mathbf{Y}_+ \sum_{k \in \mathbf{A}} e^{-jnk\omega_s T_c} + \mathbf{Y}_- \sum_{k \in \overline{\mathbf{A}}} e^{-jnk\omega_s T_c} \quad (4)$$

where both $\mathbf{Y}_+$ and $\mathbf{Y}_-$ are functions of integer $n$ and $\omega$,

$$\mathbf{Y}_\pm = \frac{1}{T_s} \int_0^{T_s} G_\pm(\omega, \tau') e^{-jn\omega_s \tau'} d\tau' \quad (5)$$

### 3.1.2 Symmetrical input ports

Because the correlator has a symmetrical structure and operates in differential mode[3], it can be modeled as a four-port network shown in Fig. 3, where P1 and P2 are the differential input ports. The impulse responses from the two symmetrical ports P1 and P2 in Fig. 3 can be grouped together to simplify the noise calculation. Let $g_+(t, \tau')$ and $g_-(t, \tau')$ stand for the impulse responses from P1, $g'_-(t, \tau')$ and $g'_+(t, \tau')$ for P2. It can be inferred that the impulse response $g_+(t, \tau')$ has the same magnitude and opposite polarity with $g'_-(t, \tau')$, as illustrated in Fig. 3. Therefore the two impulse responses for P1 and P2 are given by

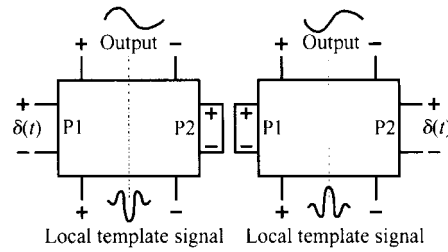


Fig. 3 Symmetric ports

$$g_1(t, \tau) = \sum_{n \in \mathbf{A}} g_+(t, \tau - nT_c) + \sum_{n \in \overline{\mathbf{A}}} g_-(t, \tau - nT_c)$$

$$g_2(t, \tau) = -\sum_{n \in \mathbf{A}} g_+(t, \tau - nT_c) - \sum_{n \in \overline{\mathbf{A}}} g_-(t, \tau - nT_c)$$

According to the above expressions and Eq. (4), the two-dimensional transfer functions for P1 and P2 can be expressed as

$$H_{1,n}(\omega) = \mathbf{Y}_+ \sum_{k \in \mathbf{A}} e^{-jnk\omega_s T_c} + \mathbf{Y}_- \sum_{k \in \overline{\mathbf{A}}} e^{-jnk\omega_s T_c} \quad (6)$$

$$H_{2,n}(\omega) = \mathbf{Y}_+ \sum_{k \in \mathbf{A}} e^{-jnk\omega_s T_c} + \mathbf{Y}_- \sum_{k \in \overline{\mathbf{A}}} e^{-jnk\omega_s T_c} \quad (7)$$

If these two noises sources at P1 and P2 are un-correlated, the output power spectrum generated by them can be summed together directly. Furthermore because the circuit is symmetrical, the PSD of the noise sources at P1 and P2 are the same with each other, which presents a more simplified method to calculate the output noise power. Using $S(\omega)$ to denote the PSD of these two noise sources and according to Eq. (2), the total output noise PSD is given by

$$T_1(\omega) = \sum_{n=0}^{\infty} S(\omega + n\omega_s) \times (|H_{1,n}(\omega)|^2 + |H_{2,n}(\omega)|^2) \quad (8)$$

For simplicity using the substitutions of $\alpha = \sum_{k \in \mathbf{A}} e^{-jnk\omega T_c}$ and $\beta = \sum_{k \in \overline{\mathbf{A}}} e^{-jnk\omega T_c}$, and then substituting Eqs. (6), (7) into (8), we obtain

$$T_1(\omega) = \sum_{n=0}^{\infty} \{ S(\omega + n\omega_s) [(|\mathbf{Y}_+|^2 + |\mathbf{Y}_-|^2) \times (|\alpha|^2 + |\beta|^2) + 4\mathrm{Re}(\mathbf{Y}_+ \mathbf{Y}_-^*) \mathrm{Re}(\alpha\beta^*)] \} \quad (9)$$

where $\mathrm{Re}(\Delta)$ means the real value of $\Delta$.

### 3.1.3 Summary

Based on the above derivation, the output noise PSD of the correlator can be calculated by: (1) Determine the PSD of the noise sources of the correlator, i.e. $S(\omega)$; (2) Calculate the impulse response and its Fourier transform for each source based on Eq. (5); (3) Calculate the output PSD for each part based on Eq. (9) and then sum them together to obtain the total output noise power.

## 3.2 Noise calculation

### 3.2.1 PSD of noise sources

The correlator can be divided into several parts to obtain the equivalent noise sources. Noticing that the four current sources and other references circuits including Q9～Q14, M1～M8, M1′～M4′ and $R_2$ in Fig. 1 are approximately independent on the LO signal, they can be represented by the equivalent current sources of $\overline{I_{n1}^2}$～$\overline{I_{n2}^2}$, $\overline{I_{n1}^2}$～$\overline{I_{n2}^2}$, as shown in Fig. 4. The common-mode feedback can be disconnected since the noise generated by the shunt-series feedback mainly comes from the feedback network itself[6]. Moreover, the transistors M5 and M6 in Fig. 1 work in the triode region and provide a small transconductance, and hence a weak feedback. The noise generated by some common components in the circuit has been allocated to two different sources. For example, the thermal noise of $R_2$ has been allocated to the sources $\overline{I_{n2}^2}$ and $\overline{I_{n2}^2}$. Thus the noises in these two sources generated by $R_2$ are correlated and should be considered when being summed together to calculate the output noise power.

If we assume that no noise enters the LO port, the noise generated by the PD cell itself can be replaced by an equivalent voltage noise source and an equivalent current noise source. Since the resistance looking into GC from $V_p^+ / V_p^-$ is much higher than looking into PD, the equivalent current source can be neglected considering its correlation with the voltage source. In order to simplify the noise calculation using the derived equation, the equivalent noise source $\overline{V_{nPD}^2}$, as shown in Fig. 4, can be divided into two serial sources, $\overline{V_{nPD+}^2}$ and $\overline{V_{nPD-}^2}$, whose amplitudes are both one half of $\overline{V_{nPD}^2}$. Thereby Equation (9) can also be utilized to calculate the output noise power by these two symmetrical sources except that they are fully correlated with each other. The other equivalent noise sources contain the base resistor thermal noise, collector current shot noise, and channel thermal noise for each transistor in PD and Q5～Q8, which are affected by the LO signal. Among them only noise sources of Q5 and Q7 are shown in Fig. 4.

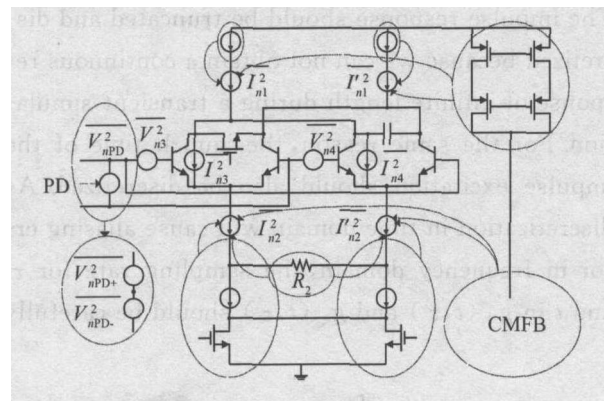


Fig. 4　Equivalent noise sources

The PSD of the equivalent noise sources $\overline{I_{n1}^2}$ and $\overline{I_{n2}^2}$ can be simulated with Cadence Spectre linear noise simulation tool and is shown in Fig. 5. The equivalent noise from $\overline{I_{n1}^2}$ mainly comes from the channel thermal noise of M1～M2, M1′～M2′, which supply the current of the GC. The reduction of both equivalent noise sources as frequency increases is due to the reduction of their gains.

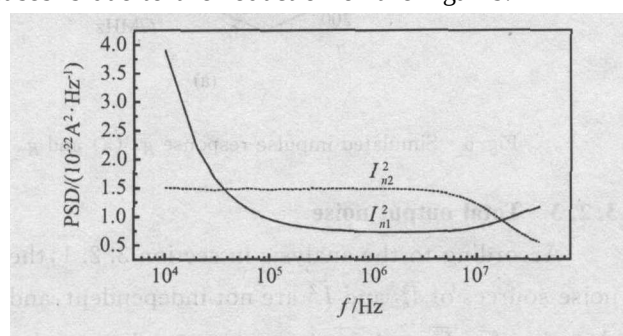


Fig. 5　Simulated PSD of $\overline{I_{n1}^2}$ and $\overline{I_{n2}^2}$

### 3.2.2 Impulse response and Fourier transform

The impulse response for each noise source at different launch time can be obtained by replacing

it with an ideal trapezoidal piecewise linear waveform generator and then taking a transient simulation. The rise time and fall time of the trapezoid piecewise linear waveform source are both taken as 1ps, and the full width of half maximum is 2ps. which ensures that the frequency spectrum of the waveform is flat enough in the duration of useful bandwidth from 3 to 10GHz and the maximal spectral deviation is only 0.002 %.

To obtain $\mathbf{Y}_+$ and $\mathbf{Y}_-$ in Eq. (5), two-dimensional Fourier transforms should be performed. The impulse response should be truncated and discretized because we can not obtain a continuous response of infinite length during a transient simulation. For the same reason, the launch time of the impulse excitation should also be discretized. As discretization in time domain will cause aliasing error in frequency domain, the sampling rate for $\tau'$ and $t$ in $g_+(t,\tau')$ and $g_-(t,\tau')$ should be carefully selected to minimize the aliasing error. In our simulation process, the discretization step is chosen as 25ps which indicates that those frequency spectrum larger than 20GHz are truncated. The difference between continuous Fourier transform and discrete Fourier transform is the sampling rate, which also has been compensated in the calculation.

Figure 6 gives the simulated impulse responses $g_+$ and $g_-$ and their two dimensional Fourier transforms. The pulse width of the LO signal is 625ps and the pulse shape is taken from Ref. [7] during simulation. Notice that the function of the circuit is correlation, which will multiply the input impulse and LO pulse and then integrate them. Therefore when the input signal is an impulse, the output of the circuit will be the same as the LO signal ideally. That is why the shape of the cross section of the impulse responses in Fig. 6 is similar to the LO pulse.

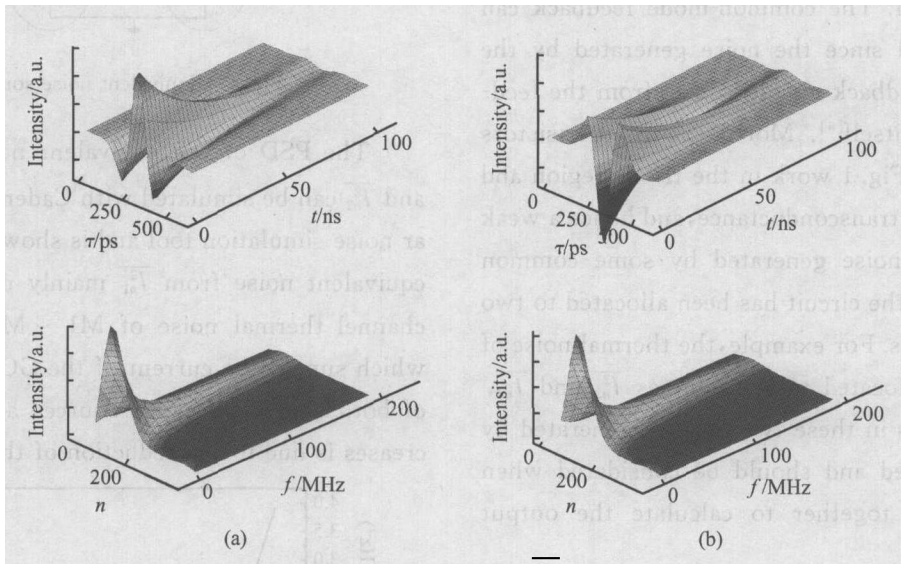


Fig. 6 Simulated impulse response $g_+$ (a) and $g_-$ (b) from $\overline{I_{n1}^2}$ and their 2-dimensional Fourier transforms

### 3.2.3 Total output noise

According to the analysis in section 3.2.1, the noise sources of $\overline{I_{n2}^2}$ and $\overline{I_{n2}^{\downarrow 2}}$ are not independent, and the same for $\overline{I_{n1}^2}$ and $\overline{I_{n1}^{\downarrow 2}}$. Let $\rho_j$ denote the correlation coefficient of the $j$th pair of the symmetrical noise sources. The total output noise power is then given by $T(\omega) = \sum_j T_j(\omega)(1+\rho_j)$, where $T_j(\omega)$ is the calculated PSD for the $j$th noise source pair based on Eq. (9).

The calculated output noises power at some selected frequency point of 4GHz for each noise source pair are listed in Table 1 and the output PSD for the correlator is shown in Fig. 7.

From the simulated results in Fig. 7, the output noise of the correlator mainly comes from the

thermal noise of the base resistor of Q5～Q8. The reason is that the base resistor noise will be amplified to the output port. In order to reduce the base resistance dual emitter stripe npn devices can be used and the periphery of the emitter that is adjacent to the base contact can also be maximized during layout design.

Table 1　Calculated output noise power at 4 GHz

| Noise source pair | $T_j(\omega)$/ ($V^2$ · $Hz^{-1}$) | ρ | Output PSD/ ($V^2$ · $Hz^{-1}$) |
|---|---|---|---|
| $\overline{I_{n1}^2}$ and $\overline{I_{n1}^2}$ | $1.01\times10^{-18}$ | 0 | $1.01\times10^{-18}$ |
| $\overline{I_{n2}^2}$ and $\overline{I_{n2}^2}$ | $7.42\times10^{-35}$ | 0.45 | $1.07\times10^{-34}$ |
| $\overline{I_{n3}^2}$ and $\overline{I_{n3}^2}$ | $3.52\times10^{-25}$ | 0 | $3.52\times10^{-25}$ |
| $\overline{V_{n3}^2}$ and $\overline{V_{n3}^2}$ | $7.15\times10^{-16}$ | 0 | $7.15\times10^{-16}$ |
| $\overline{I_{n4}^2}$ and $\overline{I_{n4}^2}$ | $6.62\times10^{-25}$ | 0 | $6.62\times10^{-25}$ |
| $\overline{V_{n4}^2}$ and $\overline{I_{n4}^2}$ | $7.15\times10^{-16}$ | 0 | $7.15\times10^{-16}$ |
| $\overline{V_{nPD+}^2}$ and $\overline{V_{nPD-}^2}$ | $2.65\times10^{-32}$ | 1 | $5.29\times10^{-32}$ |

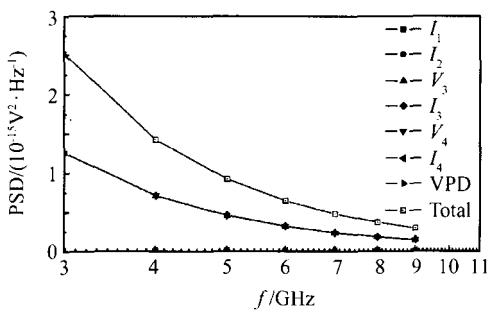


Fig. 7　Total output noise PSD

## 4　Conclusion

A new noise model for an analog correlator used in the front-end for ultra wideband communication system is investigated. The transfer function can be discretized due to the periodicity in terms of symbol of the LTV system, and the symmetrical structure of the correlator is explored to simplify the model. Specific calculations of the correlator noise are also described which gives us an insight of the noise performance of the correlator.

### References

[1] http: // developer. intel. com // technology/ itj/ q22001/ articles/ art _ 4. htm

[2] Tayler J D. Introduction to ultra-wideband radar systems. Boca Ration: CRC Press, 1995

[3] Tu Chunjiang, Liu Bo'an, Chen Hongyi. Accepted by EURASIP Jounal on Applied Signal Processing, 2004

[4] Chen C T. Linear system theory and design. Oxford, UK: Oxford University Press, 1999

[5] Hull C D, Meyer R G. A systematic approach to the analysis of noise in mixers. IEEE Trans Circuits and Systems I: Fundamental Theory and Applications, 1993, 40(12): 909

[6] Gray P R, Hurst P J, Lewis S H, et al. Analysis and design of analog integrated circuits. New York: John Wiley & Sons Inc, 2001

[7] Win M Z, Scholtz R A. Impulse radio: how it works. IEEE Comm Lett, 1998, 2(2): 36

[8] Tripathi A N. Linear systems analysis. New Delhi: Wiley Eastern Limited, 1987

### Appendix A Proof of the SVE

If there is no excitation at the RF port of the circuit and the LO port is assumed to be the input port, the system is time-invariant, and its state equation can be expressed as $d\lambda(t)/dt = A\lambda(t) + B\mathrm{LO}(t)$, where $\lambda(t)$ is the state vector, and the coefficient matrices and are both time-invariant. The solution is given by[8] $\lambda(t) = e^{At}\lambda(0) + e^{At}B\mathrm{LO}(t)$.

It can be directly derived that $\lambda(T_c)$ considering that $\lambda(0) = 0$ and $\mathrm{LO}(0) = \mathrm{LO}(T_c) = 0$. Therefore $\lambda(kT_c) = 0$, where $k$ is an integer.

From another point of view, if RF port is supposed to be the input port, the state equation of the system is then given by

$$\frac{d\lambda(t)}{dt} = C(t)\lambda(t) + D(t)\mathrm{RF}(t) \qquad (A1)$$

where $C(t)$ and $D(t)$ are time-variant. When $\mathrm{RF}(t) = 0$, i. e. the input is zero, the following equation can be derived $C(t) = d\lambda(t)/dt\,\lambda(t)$.

Therefore $C(t)$ is only dependent on the state vector $\lambda(t)$. Because $\mathrm{RF}(t)$ is random, $D(t)$ is also only dependent on the state vector of the circuit from Eq. (A1). Therefore $C(kT_c)$ and $D(kT_c)$ are both constant values. Notice that $\lambda(kT_c)$ is also constant and that the state vector $\lambda(t)$ is only dependent on its initial value, the initial values of $C(kT_c)$ and $D(kT_c)$, and the value of $\mathrm{LO}(t)$ during the $k$th chip period if $\mathrm{RF}(t) = 0$. Thereby if $\mathrm{LO}(t)$ has the same waveform during any two chips, the state vector also remains the same, i. e. $\lambda(t) = \lambda(t + kT_c)$, where $t \in [0, T_c)$ and $\mathrm{LO}(t) = \mathrm{LO}(t +$

$kT_c$). Therefore we obtain $C(t) = C(t + kT_c)$, and $D(t) = D(t + kT_c)$. Based on it, we can draw further conclusion that if the input signal waveform at the RF port is also the same in different chips, the state vector still remains the same in these chips.

# 模拟相关器的噪声分析*

涂春江 刘伯安 陈弘毅

(清华大学微电子研究所, 北京 100084)

**摘要**: 给出了分析模拟相关器的噪声模型. 将相关器分成不同的几个子模块后, 对各模块分别计算等效噪声源. 然后用理想脉冲源代替噪声源计算电路的时变传输函数, 接着用傅里叶变换计算输入输出的频域关系. 利用电路的对称结构合并对称的子模块可以进一步简化模型. 该模型可以用来估计相关器的噪声性能.

**关键词**: 噪声; 相关器; 模拟

**EEACC**: 1205; 1150

**中图分类号**: TN431.1 **文献标识码**: A **文章编号**: 0253-4177(2005)03-0480-07

*国家高技术研究发展计划资助项目(批准号:2003AA123210)

涂春江 男, 1977 年出生, 博士研究生, 主要研究方向为无线通信系统及芯片设计.

刘伯安 男, 1961 年出生, 副教授, 主要研究方向为神经网络、无线通信及其芯片设计.

陈弘毅 男, 1942 年出生, 教授, 主要研究方向为半导体器件结构和集成电路设计、ASIC 和 SOC 设计方法学、算法到硬件实现、多媒体信号处理以及信息安全.

2004-08-03 收到, 2004-10-12 定稿